

Subgap Density-of-States Extraction of Amorphous Indium-Gallium-Zinc-Oxide Thin Film Transistors by Using Multiple Frequency C-V Characteristics

Sangwon Lee, Sungwook Park, Sungchul Kim, Yongwoo Jeon, Dongsik Kong, Min-Kyung Bae, Hyun Kwang Jung, Yong Sik Kim, Dong Myong Kim, and Dae Hwan Kim^{a)}

School of Electrical Engineering, Kookmin University, 861-1, Jeongneung-dong, Seongbuk-gu, Seoul, 136-702, KOREA ^{a)}drlife@kookmin.ac.kr

Abstract

The extraction of subgap density of states (DOS) of n-channel amorphous InGaZnO (*a*-IGZO) thin film transistor (TFT) by using multi-frequency C-V characteristics is proposed and verified by the comparison of the measured I-V characteristics with the TCAD simulation results incorporating the extracted DOS. It takes on the superposition of exponential tail states and exponential deep states with following parameters $N_{TA}=1.1 \times 10^{17} [\text{cm}^{-3} \cdot \text{eV}^{-1}]$, $N_{DA}=4 \times 10^{15} [\text{cm}^{-3} \cdot \text{eV}^{-1}]$, $kT_{TA}=0.09 [\text{eV}]$ and $kT_{DA}=0.4 [\text{eV}]$. In addition, it is shown that the extracted subgap DOS is independent of the channel length and width of *a*-IGZO TFTs. Proposed technique makes it possible to gain the frequency-independent C-V curve which is very useful for oxide semiconductor TFT modeling and characterization and takes the nonlinear relation between the energy level of DOS and the gate voltage V_{GS} into account. In addition, it is the simple, fast, and accurate extraction method of DOS without optical illumination, temperature-dependence, and numerical calculations.

I. Introduction

In recent years, amorphous Indium-Gallium-Zinc-Oxide (*a*-InGaZnO) thin film transistors (TFTs) have emerged as promising candidates substituting a-Si:H and/or low temperature poly-Si (LTPS) TFTs as switching/driving devices for active-matrix liquid crystal displays (AMLCDs) and active-matrix organic light-emitting diodes (AMOLEDs) due to the advantages of large area uniform integration, a low cost room temperature fabrication process, a high mobility, and the compatibility with transparent, flexible, and light display applications [1]. Since subgap density of states (DOS: $g(E)$) of *a*-InGaZnO film is one of most important parameters determining both the electrical characteristics and the reliability, the extraction of subgap DOS of *a*-InGaZnO TFTs based on various techniques have been pursued by many research groups. Hsieh, Kimura, and co-authors extracted DOS by the numerical simulation-based fitting, where the influence of free carrier density was assumed to be negligible [2, 3]. Jeon, Park, and co-authors have demonstrated the DOS extraction based on optical response of capacitance-voltage (C-V) characteristics [4, 5]. However, if the parameter extraction for display applications is deliberated, in order to characterize the instabilities of TFTs under illumination by backlight environment, the DOS extraction technique by employing additional photons becomes undesirable because it can be a destructive extraction scheme in case that the electrical characteristics of TFTs are changed only under an optical illumination. More recently, Chen and co-authors reported the DOS extraction based on Meyer-Neldel rule of activation energy [6], which is too complex to apply to the practical extraction of reliability-related DOS parameters because the temperature dependence is necessary to be measured. Motivated by these backgrounds, in this work, the extraction of subgap DOS in *a*-InGaZnO TFT by using multi-frequency C-V characteristics is proposed and demonstrated. Proposed technique makes it possible to gain the frequency (f)-independent C-V curve which is very useful for TFT modeling and characterization. In addition, it has no need of optical illumination, temperature-dependence, and numerical calculations.

II. Device Structure

The device structure used in this work is of the inverted staggered type which is the most commonly used structure for AMLCD. Devices are fabricated as follows: On a thermally grown SiO_2/Si substrate, the first sputtered deposition at RT and patterning of molybdenum (Mo) gate are followed by plasma-enhanced chemical vapor deposition (PECVD) of SiO_2 ($T_{OX}=100 \text{ nm}$) at 300 °C. An *a*-IGZO film ($\text{In}_2\text{O}_3:\text{Ga}_2\text{O}_3:\text{ZnO}=2:2:1$ at %) is then

sputtered by RF magnetron sputtering at RT in a mixed Ar/ O_2 (100:1 at sccm) and wet-etched with diluted HF to get the pattern of 70-nm-thick active layer ($T_{IGZO}=70 \text{ nm}$). To form S/D electrode, a 200-nm-thick layer of Mo is sputtered at RT and then patterned by dry-etching. After N_2O plasma treatment, a SiO_2 passivation layer is continuously deposited at 150 °C by PECVD without a vacuum break. The channel length (L), the channel width (W), and the length of the overlap region between the gate and S/D (L_{ov}) are designed to be 40~50, 50~200, and 10 μm , respectively.

III. Characterization of C-V Characteristics

The measurement setup is illustrated in Fig. 1(a). Inherent frequency-dependence of C-V curve in AOS TFTs results from the partial response of trapping/detrapping dynamics of subgap DOS to small signal in V_G . As shown in Fig. 1(b), the *a*-IGZO C-V curve from LCR meter is so sensitive to a small signal frequency that huge error in characterizing interface/bulk traps by using conventional extraction method based on the frequency-dependence (e.g., charge pumping or conductance method) is likely to arise. In order to circumvent this hurdle, the evolution from 2-element model of LCR meter to frequency-independent gate capacitance model [7, 8] via 4-element model is proposed and demonstrated as illustrated in Fig. 2 and Table I. By embedding C_{LOC} (small signal-responsive *a*-IGZO localized charge Q_{LOC}), R_L (frequency-independent resistance for the extension from 4-element model), and C_{FREE} (small signal responsive *a*-IGZO free charge Q_{FREE}) in the impedance Z_{IGZO} (Fig. 3(c)), we can describe the frequency-dependent C-V curve with the physically meaningful parameters. For convenience, R_S is extracted from the saturated magnitude Z_M in MHz range (as seen in the inset of Fig. 3(a)). Consequent V_G -dependent R_S in Fig. 3(a) is within the consistent range with previous work [9]. On the condition of $Z_M=Z_{CH}$ (Eq. (1)~(5)) and $Z_{CH}=Z_{IGZO}$ (Eq. (6)~(8)), the unique solutions of frequency-independent gate capacitance (C_{LOC} and C_{FREE} in Fig. 9(d)) can be found by using (6)~(8) and measured C-V curves at three different frequencies (1, 2, and 3). Conclusively, the final C_G in Fig. 2(d) is extracted by using the proposed multi frequency method as the wide range frequency independent parameter as shown in Fig. 3(b). Taking into account that C_{LOC} reflects the V_G -dependent Q_{LOC} , DOS can be extracted by using Eq. (11)~(14) as seen in Fig. 4(a). Fig. 4(b) shows DOS extracted in *a*-IGZO TFTs with different W/L ($W=200, 100, 50 \mu\text{m}$ and $L=40 \mu\text{m}$). It is independent of the channel length and width of *a*-IGZO TFTs.

Extracted DOS is incorporated into TCAD model [9] and verified by comparing TCAD simulation result with the measured I-V characteristics as shown in Fig. 5. Our results show that the extracted DOS-based TCAD model reproduces very well measured I-V curves under wide range of bias.

V. Conclusions

The extraction of subgap DOS in *a*-InGaZnO TFT by using multi-frequency C-V characteristics is proposed and verified by the comparison of the measured I-V characteristics with the TCAD simulation results incorporating the extracted $g(E)$. Proposed technique makes it possible to gain the f -independent C-V curve which is very useful for TFT modeling and characterization and takes the nonlinear relation between E and V_{GS} into account. In addition, it makes the simple, fast, and accurate extraction of subgap DOS possible without optical illumination, temperature-dependence, and numerical calculations.

Acknowledgements

This work was supported by the Korea Science and Engineering Foundation (KOSEF) grant funded by the Korea government (MEST) (No. 2009-0080344).

References

- [1] J. Y. Kwon et al, IEEE Electron Device Lett., 29 1309 (2008)
- [2] H.-H. Hsieh et al, Appl. Phys. Lett., 92 133503-1(2008)
- [3] M. Kimura et al, Appl. Phys. Lett., 92, 133512-1 (2008)
- [4] K. Jeon, et al, Appl. Phys. Lett., 93, 182102-1 (2008)
- [5] J.-H. Park et al, IEEE Electron Device Lett., 29, 1292 (2008)
- [6] C. Chen et al, IEEE Transactions on Electron Dev., 56, 1177 (2009).
- [7] Z. Luo et al., IEEE Electron Device Lett. 25, 655 (2004)
- [8] K. J. Yang et al., IEEE Trans. Electron Devices. 46, 1500 (1999)
- [9] J. Park et al., IEEE Electron Device Lett. 29, 879 (2008)

Table I. Multi-frequency C - V method equations for extracting DOS of a -IGZO TFTs

Conversion from 2-element model to 4-element model ($Z_M = Z_{CH}$)	
$Z_M = \frac{R_M}{1 + (\omega C_M R_M)^2} - \frac{j\omega C_M R_M^2}{1 + (\omega C_M R_M)^2}$	(1)
$Z_{CH} = R_S + \frac{R_{CH}}{1 + (\omega C_{CH} R_{CH})^2} - j \left(\frac{\omega C_{CH} R_{CH}^2}{1 + (\omega C_{CH} R_{CH})^2} + \frac{1}{\omega C_{OX}} \right)$	(2)
$R_S = \frac{D_M}{\omega C_M (1 + D_M^2)} - \frac{R_{CH}}{1 + (\omega C_{CH} R_{CH})^2}; D_M = \frac{1}{\omega C_M R_M}$	(3)
$R_{CH} = \sqrt{\frac{C_M (1 + D_M^2) - C_{OX}}{\omega^2 C_{CH}^2 C_{OX} - \omega^2 C_{CH} C_M (1 + D_M^2) (C_{CH} + C_{OX})}}$	(4)
$C_{CH} = \frac{b C_{OX}^2 - b^2 C_{OX}}{\{(ab\omega)^2 + 1\} C_{OX}^2 - 2b C_{OX} + b^2};$	(5)
$a = \frac{R_M}{\omega C_M (1 + D_M^2)} - R_S, b = C_M (1 + D_M^2)$	
M : Impedance in 2-element model. Z_{CH} : Impedance in 4-element model R_S : Series resistance of a -IGZO TFTs R_{CH} : Frequency dependent channel resistance in 4-element model C_{CH} : Frequency dependent channel capacitance in 4-element model	
Conversion from 4-element model to Equivalent model of a -IGZO TFTs ($Z_{CH} = Z_{IGZO}$)	
$Z_{IGZO} = \frac{C_{LOC}^2 R_L^2}{\omega^2 C_{LOC}^2 C_{FREE}^2 R_L^2 + (C_{LOC} + C_{FREE})^2} - j \frac{\omega^2 C_{LOC}^2 C_{FREE} R_L^2 + (C_{LOC} + C_{FREE})}{\omega^3 C_{LOC}^2 C_{FREE}^2 R_L^2 + \omega (C_{LOC} + C_{FREE})^2}$	(6)
$R_L = \frac{1}{\omega C_{LOC}} \sqrt{\frac{\omega^2 C_{CH} R_{CH}^2 (C_{LOC} + C_{FREE}) (C_{LOC} + C_{FREE} - C_{CH}) - (C_{LOC} + C_{FREE})}{C_{FREE} (1 + \omega^2 C_{CH} R_{CH}^2 (C_{CH} - C_{FREE}))}}$	(7)
$R_L(\omega_1) = R_L(\omega_2) = R_L(\omega_3)$	(8)
$C_{CH} = C_{FREE} + \frac{C_{LOC}}{1 + \omega^2 \tau_{LOC}^2}; \tau_{LOC} = C_{LOC} \times R_L$	(9)
$\frac{R_{CH}}{\omega} = \frac{C_{LOC} \omega \tau_{LOC}}{1 + \omega^2 \tau_{LOC}^2}$	(10)
Z_{IGZO} : Equivalent Impedance of a -IGZO TFTs R_L : Frequency independent resistance related to the frequency-dependent C - V characteristic in 2-element model	
DOS extraction from C_{LOC}	
$C_{LOC} = (C_{LOC}(V_{GS1}) - C_{LOC}(V_{GS2})) / (W \times L \times T_{IGZO})$	(11)
$g(E) = \frac{C_{LOC}}{q^2} = N_{TA} \times \exp\left(-\frac{(E_C - E)}{KT_{TA}}\right) + N_{DA} \times \exp\left(-\frac{(E - E_V)}{KT_{DA}}\right)$	(12)
$V_G = V_{FB} + \phi_s + \frac{Q_{LOC} + Q_{FREE}}{C_{OX}}$	(13)
$\phi_s = \int_{V_{FB}}^{V_G} \left(1 - \frac{C_G}{C_{OX}}\right) dV_G$	(14)

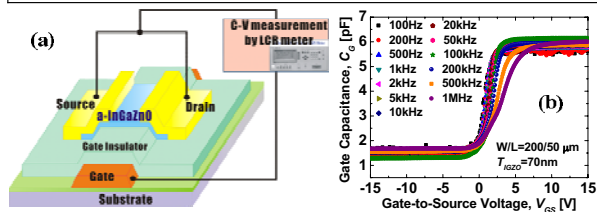


Fig. 1. (a) Frequency-dependent C - V curves measured with LCR meter (HP 4284) and (b) frequency-independent C - V curves

extracted by using multi-frequency C - V method.

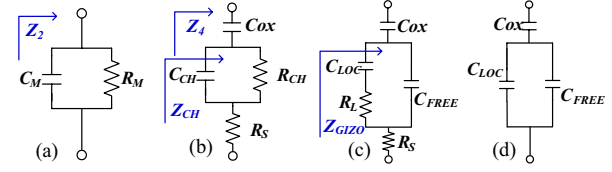


Fig. 2 (a) 2-element model of LCR meter, (b) 4-element model, (c) equivalent capacitance model of a -IGZO TFTs and (d) frequency independent gate capacitance model.

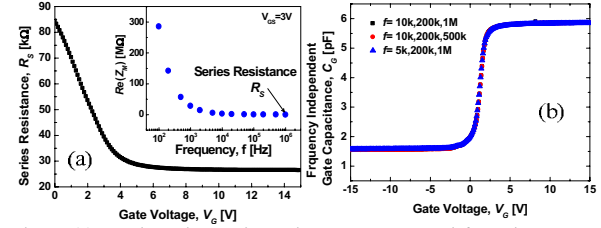


Fig. 3. (a) V_{GS} -dependent series resistance R_S measured from the saturated $Re(Z_M)$ in high frequency (LCR meter) and (b) frequency-independent C - V curves extracted by using multi-frequency C - V method.

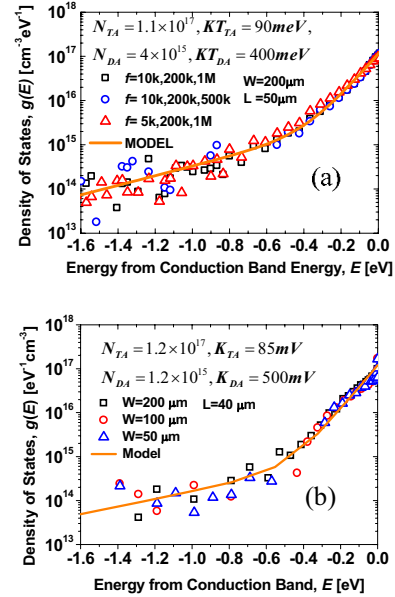


Fig. 4. (a) DOS extracted from C_{LOC} under the proposed multi-frequency method by using Fig. 3(b) and Eq. (11)–(14), (b) DOS extracted in a -IGZO TFTs with different W/L ($W=200, 100, 50 \mu\text{m}$ and $L=40 \mu\text{m}$).

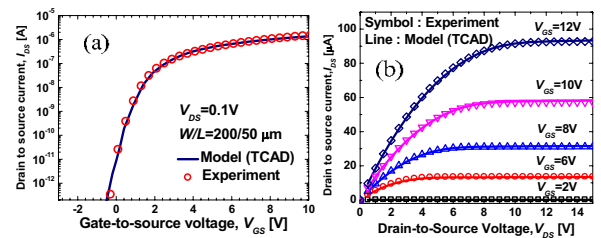


Fig. 5. Comparison between the measured I - V and TCAD I - V characteristics. TCAD I - V curve is calculated by incorporating the extracted DOS (Fig. 11(b)) into TCAD model. (a) Transfer curve and (b) output curve. The extracted DOS-based TCAD model agrees very well with measured characteristics.